

## Supporting information

### **The Gas Diffusion Electrode Setup as Straightforward Testing Device for Proton Exchange Membrane Water Electrolyzer Catalysts**

Johanna Schröder<sup>a</sup>, Vladislav A. Mints<sup>a</sup>, Aline Bornet<sup>a</sup>, Etienne Berner<sup>a</sup>, Mohammad Fathi Tovini<sup>b</sup>, Jonathan Quinson<sup>c</sup>, Gustav K. H. Wiberg<sup>a</sup>, Francesco Bizzotto<sup>a</sup>, Hany A. El-Sayed<sup>b</sup>, Matthias Arenz<sup>a\*</sup>.

<sup>a</sup> Department of Chemistry, Biochemistry and Pharmaceutical Sciences, University of Bern, Freiestrasse 3, 3012 Bern, Switzerland

<sup>b</sup> Chair of Technical Electrochemistry, Department of Chemistry and Catalysis Research Center, Technical University Munich, Lichtenbergstrasse 4, 85748 Garching, Germany.

<sup>c</sup> Department of Chemistry, University of Copenhagen, Universitetsparken 5, 2100 Copenhagen, Denmark.

<b>Experimental</b> .....	3
<i>Chemicals, materials, and gases</i> .....	3
<i>Gas diffusion electrode setup</i> .....	3
<i>Rotating disk electrode setup</i> .....	6
<i>Ink formation</i> .....	6
<i>Catalyst film preparation</i> .....	6
Vacuum filtration and pressing of GDE .....	6
Film preparation with PTL.....	7
RDE film preparation.....	7
<i>Electrochemical measurements</i> .....	8
Electrochemical measurements in GDE setup .....	8
Electrochemical measurement in RDE setup.....	8
<i>Characterization</i> .....	9
Determination of the OER overpotential .....	9
X-ray photoelectron spectroscopy (XPS) .....	10
Scanning electron microscope (SEM) and energy-dispersive X-ray spectroscopy (EDS) .....	10
Transmission electron microscopy (TEM).....	10
<b>OER activity measurements</b> .....	11
<i>GDE and RDE data</i> .....	11
<i>Tafel plot determination</i> .....	13
<i>Exchange current density and activation energy</i> .....	14
<b>XPS and TEM measurement</b> .....	17
<b>References</b> .....	17

## Experimental

### *Chemicals, materials, and gases*

For the catalyst ink formation, dilution of the acid, and the cleaning of the GDE cell ultrapure Milli-Q water (resistivity  $> 18.2 \text{ M}\Omega \cdot \text{cm}$ , total organic carbon (TOC)  $< 5 \text{ ppb}$ ) from a Millipore system was used. For the preparation of the catalyst inks isopropanol (IPA, 99.7+ %, Alfa Aesar), glycerol (sigma, for molecular biology,  $\geq 99 \%$ ), commercial  $\text{IrO}_2$  (Alfa Aesar, Iridium(IV) oxide, Premion®, 99.99% metals basis, Ir 84.5% min, MFCD00011065) and Nafion dispersion (D1021, 10 wt.%, EW 1100, Fuel Cell Store) were used.

The GDE was prepared using a Nafion membrane (Nafion 117, 183  $\mu\text{m}$  thick, Fuel Cell Store), two carbon gas diffusion layers (GDL) (Freudenberg H23, 0.210 mm thick, Fuel Cell Store; with a microporous layer (MPL): Freudenberg H23C8, 0.230 mm thick), a porous transport layer (PTL) (Sintered titanium, Mott Corporation, USA) and Teflon (polytetrafluorethylene, PTFE) spray (BOLA Fluorkunststoff spray, Bohlender). The used Nafion membrane was always pretreated. Cutoff membranes (diameter of 2 cm) were treated in 5 wt.%  $\text{H}_2\text{O}_2$  (Hänseler, 30 min, 80 °C), rinsed with Milli-Q water, treated in Milli-Q water (30 min, 80 °C), again rinsed with Milli-Q water, treated in 8 wt.%  $\text{H}_2\text{SO}_4$  (30 min, 80 °C) and finally rinsed with Milli-Q water. Afterwards the cutoff membranes were stored in a with Milli-Q water filled glass vial.

The electrochemical measurements were performed using diluted 70% perchloric acid ( $\text{HClO}_4$ , GDE: 99.999% trace metals basis, Sigma Aldrich; RDE: Suprapur, Merck) as electrolyte and the gas argon (Ar) or oxygen ( $\text{O}_2$ ) from Air Liquide (99.999 %).

### *Gas diffusion electrode setup*

For the electrochemical measurements an in-house developed GDE setup was used. The GDE was placed above a flow-field of a Polychlorotrifluoroethylene (PCTFE) cell body with the Nafion membrane upwards. The upper cell part made of Teflon was placed above the Nafion membrane. Two Au pins (Conrad Electronic, 1025-M-1.5N-AU-1.5) were placed vertical inside the cell body and a plastic disk as base was screwed into the cell body to push the Au pins into the GDE. Two screws were used to enable an electric contact via Au pins to the GDE (i.e. working electrode (WE)). The previously stainless steel lower cell body<sup>1</sup> was for this study replaced by PCTFE. The main advantages of this replacement are the higher chemical resistance due to prevention of corrosion of the cell body (by acid and water) that in the past sometimes led to iron signals during potentiodynamic measurements. While the corrosion of

the flow field was easily visible and could be removed by a fast grinding the rusting of the internal parts (from gas inlet to outlet) was really challenging. Therefore, the high chemical resistance of PCTFE against  $\text{HClO}_4$  is an important improvement. The only corroding components in the new setup are the easily replaceable Au pins.

A platinum wire was used as a counter electrode (CE) and a reversible hydrogen electrode (RHE) as a reference electrode (RE). The CE was placed inside a glass capillary with a glass frit on the bottom to avoid the trapping of gas bubbles in the hole of the Teflon cell and thus helping to improve the reproducibility of the measurement. The CE inside the frit and the RE were placed in the upper cell part inside the electrolyte. The position of the CE was fixed with a holder to keep a constant position and preventing the falling out of the upper cell part. All potentials in this study are referred to the RHE potential.

The Teflon upper cell body was initially cleaned by soaking it overnight in acid ( $\text{H}_2\text{SO}_4:\text{HNO}_3 = 1:1, \text{v:v}$ ) following by rinsing and twice boiling in ultrapure water. Between measurements, it was boiled once in ultrapure water together with the RE, and the glass capillary.

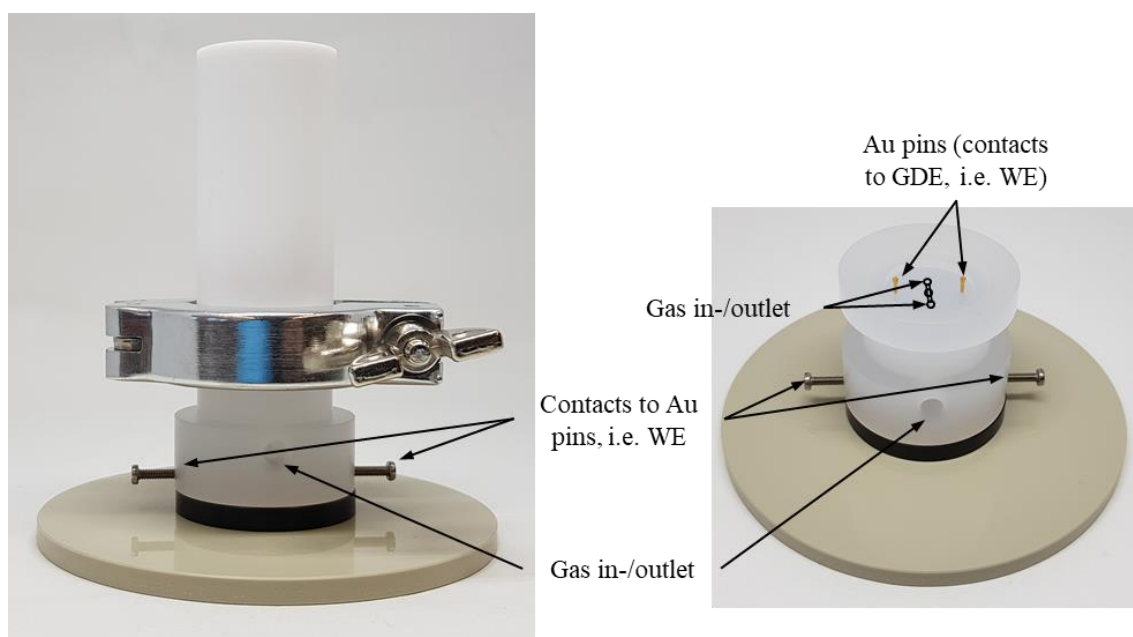


Figure S1. Pictures of the developed GDE setup for OER measurements consisting of a PCTFE cell body, two screws as contacts to the Au pins, i.e. the WE, and a PTFE upper cell body.

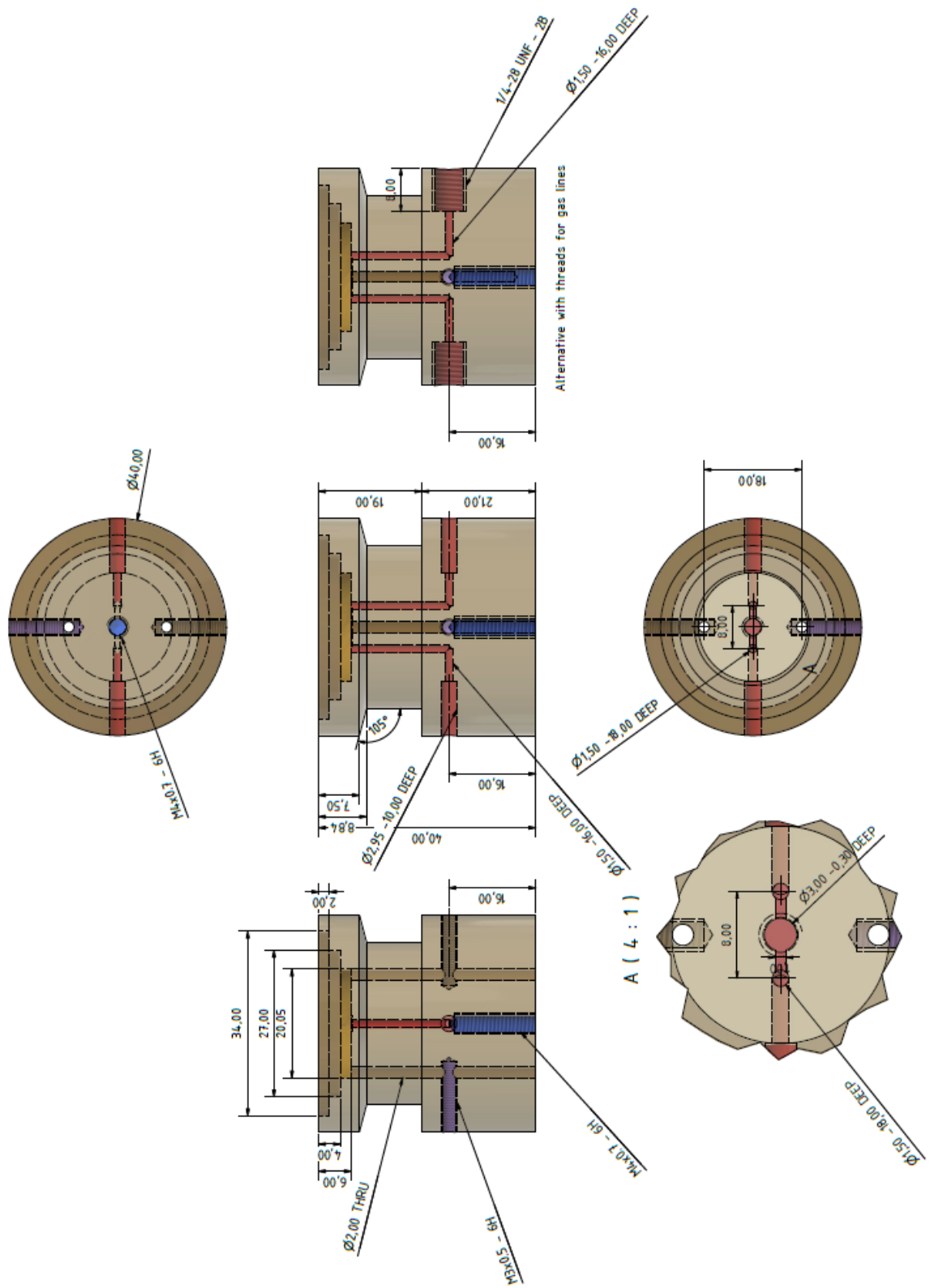


Figure S2. Technical drawing of the GDE setup.

### ***Rotating disk electrode setup***

The RDE experiments were carried out in a three-electrode glass cell setup. For the 60 °C measurement a glass jacket cell setup was used. A trapped hydrogen RHE electrode serves as a RE and a platinum mesh served as CE. The RE was separated from the working compartment via a Luggin capillary to reduce the iR drop, whereas the CE was separated with a zirconia frit to prevent hydrogen crossover.

### ***Ink formation***

For RDE and the GDL film preparation the catalyst was dispersed in a mixture of Milli-Q water and IPA (water/IPA ratio of 3:1). For the GDE film preparation an Ir concentration of 14 mg<sub>Ir</sub> mL<sup>-1</sup> and for the RDE of 654 μg<sub>Ir</sub> mL<sup>-1</sup> was used. To obtain a suitable dispersion the mixture was sonicated for 10 min in a sonication bath (inks for GDE) or horn sonicator (inks for RDE). Nafion was added to the ink for the GDE to reach 10 wt.% with regard to the catalyst and the dispersion was again sonicated for 10 min in a sonication bath.

For the PTL film preparation the catalyst was dispersed in a glycerol ink using a concentration of 28 mg<sub>Ir</sub> mL<sup>-1</sup>. 2.5 g glycerol and 69.5 μL of Nafion (to reach 10 wt % with regard to the catalyst) were stirred (680 rpm) for 30 min (glass vial was covered in aluminum foil). 46.5 mg of catalyst and 1.75 g of the glycerol-Nafion mixture was stirred (1200 rpm) for 30 min (glass vial was covered in aluminum foil).

### ***Catalyst film preparation***

#### Vacuum filtration and pressing of GDE

The Freudenberg H23C8 carbon gas diffusion layer (GDL) was placed between a glass funnel and a sand core filter (diameter 1.5 cm) in a vacuum filtration setup. This was placed on a collecting bottle as described by Yarlagadda et al.<sup>2</sup> 0.506 (0.253, or 0.126) mL of the inks of the commercial catalyst were diluted with 3.155 (1.580, or 0.789) mL of Milli-Q water and 10.476 (5.238, or 2.620) mL of IPA (water-IPA ratio of 1:3, Ir concentration of 0.5 mg<sub>Ir</sub> mL<sup>-1</sup>). The mixture was sonicated for 1 min. The diluted ink was filled in a funnel. A membrane water pump was used to deposit the catalyst on top of the GDL. The GDE was dried at least overnight on air. By this procedure theoretical Ir loading of 4 (2, or 1) mg<sub>Ir</sub> cm<sup>-2</sup><sub>geo</sub> was generated.

The Nafion membrane was pressed on top of the GDE: A Teflon or paper sheet was placed on top of a Teflon block and afterwards a GDL with MPL (Ø 2 cm with hole of Ø 3 mm) and the catalyst deposited on the GDL by vacuum filtration (Ø 3 mm) into the hole. A Nafion

membrane (to avoid later the leaking of the electrolyte into the GDE) was rinsed with Milli-Q water, dried and followed by a second Teflon sheet and a second Teflon block placed on top. Everything was placed between two metal blocks and the pressing was performed at 2 tons for 10 min. Afterwards the pressed GDE was placed on top of the GDL without MPL ( $\varnothing$  2 cm) in the cell body (see Figure S3). The second GDL was not pressed together with the other parts of the WE as sometimes it stuck to the Teflon sheets leading to nonuniform thicknesses of the GDLs. The additional GDL was placed so that the WE (of 3 mm diameter) remained in position and did not fall down what would lead to a loss in connection. As the WE was only pressed but not under increased temperature (i.e. no hot-pressing) in previous experiments it sometimes did not stay in the middle of the hole of the upper GDL.

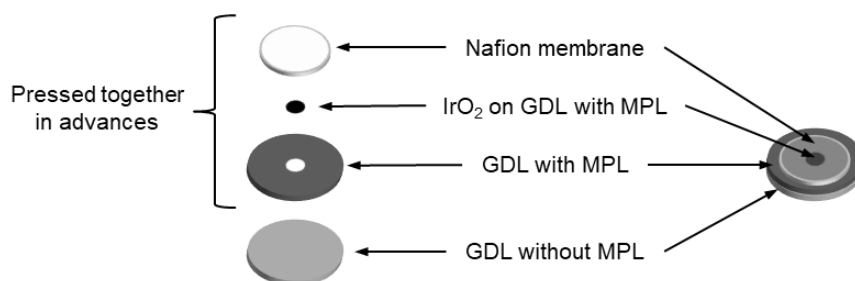


Figure S3. Illustration of the arrangement of the GDLs used in this study

#### Film preparation with PTL

Teflon spray was sprayed on PTL cutoffs ( $\varnothing$  2 cm) and dried under a hood. Afterwards 2.52  $\mu\text{L}$  of 28  $\text{mg}_{\text{Ir}} \text{mL}^{-1}$  of the glycerol-based ink was drop casted in the middle of the PTL disk and placed on a glass petri dish for 13.5 h at 135  $^{\circ}\text{C}$  in an oven.

The Nafion membrane was pressed in a simple homemade hot-pressing setup on the PTL: An aluminum foil was placed in a metal autoclave reactor, the Nafion membrane on top of the PTL (catalyst film upside) and a second aluminum foil was added. The pressing was performed by pressing a metal piece on top of the aluminum foil with a metal screw-tube combination by closing three screws of the metal cap. The pressing setup was placed for 5 min on a hot plate of 135 $^{\circ}\text{C}$ .

#### RDE film preparation

The alkaline ink was mixed for 5 min using an Ultra Turrax (IKA, T18 digital) at 20'000 rpm. 14.98  $\mu\text{L}$  of the ink were drop casted onto the glassy carbon (GC) disk to achieve a theoretical

loading of  $50 \mu\text{g}_{\text{Ir}} \text{cm}^{-2}_{\text{geo}}$ . The electrodes were then dried under humidified ( $\text{H}_2\text{O}/\text{IPA}$  ratio of 3:1) Ar flow.

### ***Electrochemical measurements***

#### **Electrochemical measurements in GDE setup**

For the electrochemical measurements, a computer controlled parallel potentiostat (ECi-242, NordicElectrochemistry ApS) was used. The gas was humidified by passing a bubbler filled with Milli-Q water and the gas inlet was connected to the cell body. The gas flow rate was determined with a mass flow controller (7000 flowmeter, Ellutia Chromatography Solutions). As electrolyte 4 M  $\text{HClO}_4$  aqueous solution were used in the upper Teflon compartment of the GDE and different temperatures (30, 40, 50, or 60 °C) were applied using a fan in an isolated Faraday cage. After assembling the setup, one or two cyclic voltammograms (CV) were recorded while purging the electrode with humidified gas (with a scan rate of  $10 \text{ mV s}^{-1}$ , 1.2-1.6  $V_{\text{RHE}}$ ) to check if the assembling of the cell was successful. Afterwards humidified gas was purged for 10-20 min to reach the desired temperature before starting any experiments. For guaranteeing the complete oxidation of the Ir based catalyst the electrode potential was hold at 1.6  $V_{\text{RHE}}$  for 5 min. Before starting the measurement, a current of  $1 \text{ mA mg}_{\text{Ir}}^{-1}$  was applied for 5-10 min. The measurement series consisted of current steps with 2 or 5 min holding per current. Different current densities were applied: 1, 2.5, 5, 7.5, 10, 12.5, 15, 20, and 25  $\text{mA mg}_{\text{Ir}}^{-1}$  for temperature dependent measurements (30-60 °C); 1, 5, 10, 20, 30, 40, 50, 60, 70, 85, 100, 125, and 150  $\text{mA mg}_{\text{Ir}}^{-1}$  for 60 °C measurements ( $\text{O}_2$  vs. Ar atmosphere, GDL vs. PTL substrate); 0.25, 1.25, 2.5, 5, 7.5, 12.5, and 17, 5  $\text{mA mg}_{\text{Ir}}^{-1}$  for 40 °C measurements in Ar. The resistance during the measurement was determined online using an AC signal (5 kHz,  $5 \times 10^{-5} \text{ A}$ )<sup>3</sup>. The activity was analyzed of the iR corrected data averaging the potential of the last 60 s (of 2 min holding) or last 100 s (of 5 min holding) of each current step. Each measurement was repeated three times with a new WE and setup.

#### **Electrochemical measurement in RDE setup**

The potential and current are measured with a computer controlled potentiostat. As standard an electrolyte of 0.1 M  $\text{HClO}_4$  was used.

Care needs to be taken to keep the electrochemical cell clean. A suitable procedure is to store in between the experiments the glassware in acidic  $1 \text{ g L}^{-1} \text{ KMnO}_4$  solution. Prior to the experiments this solution is removed, and the glassware rinsed with a diluted  $\text{H}_2\text{SO}_4/\text{H}_2\text{O}_2$



solution to remove residual MnO<sub>2</sub>. Finally, the glassware is boiled three times in ultrapure water.

During measurement, the cell is degassed by bubbling O<sub>2</sub> through the solution for 20 minutes prior to the start of the experiment. This O<sub>2</sub> flow is also maintained throughout the whole experiment. The WE is inserted into the solution under potentiostatic control at 1.0 V<sub>RHE</sub>.

As the potentiostat has an active iR compensation scheme such as positive feedback, the iR drop in the cell is adjusted first. For this the potential is kept at 1.0 V<sub>RHE</sub>, and the impedance resistance at 5 kHz with 5 mV amplitude is measured. This measured resistance is then reduced to 5 ohms by adjusting the feedback loop of the potentiostat. Afterwards an electrochemical impedance spectrum (EIS) is taken between 1 Hz to 50 kHz with an amplitude of 5 mV to evaluate the apparent solution resistance. If the potentiostat has no active iR compensation only the latter step (EIS) is taken. The solution resistance from the impedance spectrum is employed to post-correct the data for the iR drop.

In the following step the electrode is activated by holding it at 1.65 V<sub>RHE</sub> for 10 minutes at a RDE rotation of 3600 rpm. This activation is important to completely oxidize the catalyst and avoid additional oxidation current during OER evaluation that could be misinterpreted as activity.

The rotation is maintained until all electrochemical experiments are finished. After the activation, 5 consecutive CV cycles at 10 mV s<sup>-1</sup> between 1.0 and 1.6 V<sub>RHE</sub>. When the CVs were finished, a potentiostatic experiment is performed, in which each potential is hold for 2 minutes. The potentials are: 1.0, 1.1, 1.2, 1.3, 1.4, 1.45, 1.475, 1.5, 1.525, 1.55, 1.575, 1.6, 1.575, 1.55, 1.525, 1.5, 1.475, 1.45, 1.4, 1.3, 1.2, 1.1, 1.0 V<sub>RHE</sub>. Following this experiment 3 CV cycles between 1.0 and 1.6 V<sub>RHE</sub> are measured at 10 mV s<sup>-1</sup>.

## ***Characterization***

### Determination of the OER overpotential

For temperature dependent measurement the potential versus RHE was converted to the OER overpotential:

$$\eta_{\text{OER}} = E_{\text{rev},T} - E_{\text{RHE}}$$

For the determination of the reversible potential the equation of Parthasarathy et al.<sup>4</sup> was used (calories were converted into joules) with T as temperature (in K), n = 2 transferred electrons to produce one mol of water, F as Faraday constant:

$$E_{\text{rev},T} = \frac{-\Delta G^0}{n F} = \frac{295600 + 33.5 T \ln(T) - 388.4 T}{n F}$$

### X-ray photoelectron spectroscopy (XPS)

XPS was performed on a Kratos Axis Supra spectrometer using monochromatic Al K $\alpha$  radiation at an energy of 1486.6 eV. The spectra were recorded at a total power of 225 W, 15 kV and 15 mA anode current. Pristine IrO $_2$  catalysts were drop-casted on a copper tape in a floating mode on a stainless-steel sample bar and then outgassed during overnight in an ultrahigh vacuum chamber so that the pressure in the chamber during the analysis was less than  $1.0 \times 10^{-8}$  Torr. The catalyst coated GDEs with a loading of  $2 \text{ mg}_{\text{Ir}} \text{ cm}_{\text{geo}}^{-2}$  after activity measurement were grinded into powder by a mortar and pestle and drop-casted the same way as the raw catalysts for the XPS analysis. The narrow Ir 4f spectra were collected using a step size of 0.05 eV, a pass energy of 20 eV and the represented data are the average of 10 recorded spectra. All the binding energy values are corrected using the carbon signal (C 1s = 284.8 eV).

### Scanning electron microscope (SEM) and energy-dispersive X-ray spectroscopy (EDS)

After performing the oxidation step of the catalyst with a loading of  $2 \text{ mg}_{\text{Ir}} \text{ cm}_{\text{geo}}^{-2}$ , a circle of 5 mm was punched around the GDE as described before.<sup>5</sup> The dried sample was detached from the Nafion membrane and fixed with Cu-adhesive tape (3M #1182 electrical tape) on the sample holder. Before cutting with a scalpel the coated GDL was dipped for 10 s in liquid nitrogen.

The measurements of the cross-section were performed on a Zeiss GeminiSEM 450 using SmartSEM 6.05 software with EDS Photodetector Ultim max 65 from Oxford instruments using AZTec 4.2 software. As scan parameters for the EDS maps a WD (working distance) of 8.8 mm, accelerating voltage of 15 kV and a probe current of 200 pA were used.

### Transmission electron microscopy (TEM)

TEM was performed using a Jeol 2100 microscope operated at 200 kV. The sample was prepared by drop casting a dispersion of the IrO $_2$  catalyst on carbon coated copper grids (300 mesh grids, Quantifoil) and dried in air at room temperature.

## OER activity measurements

### GDE and RDE data

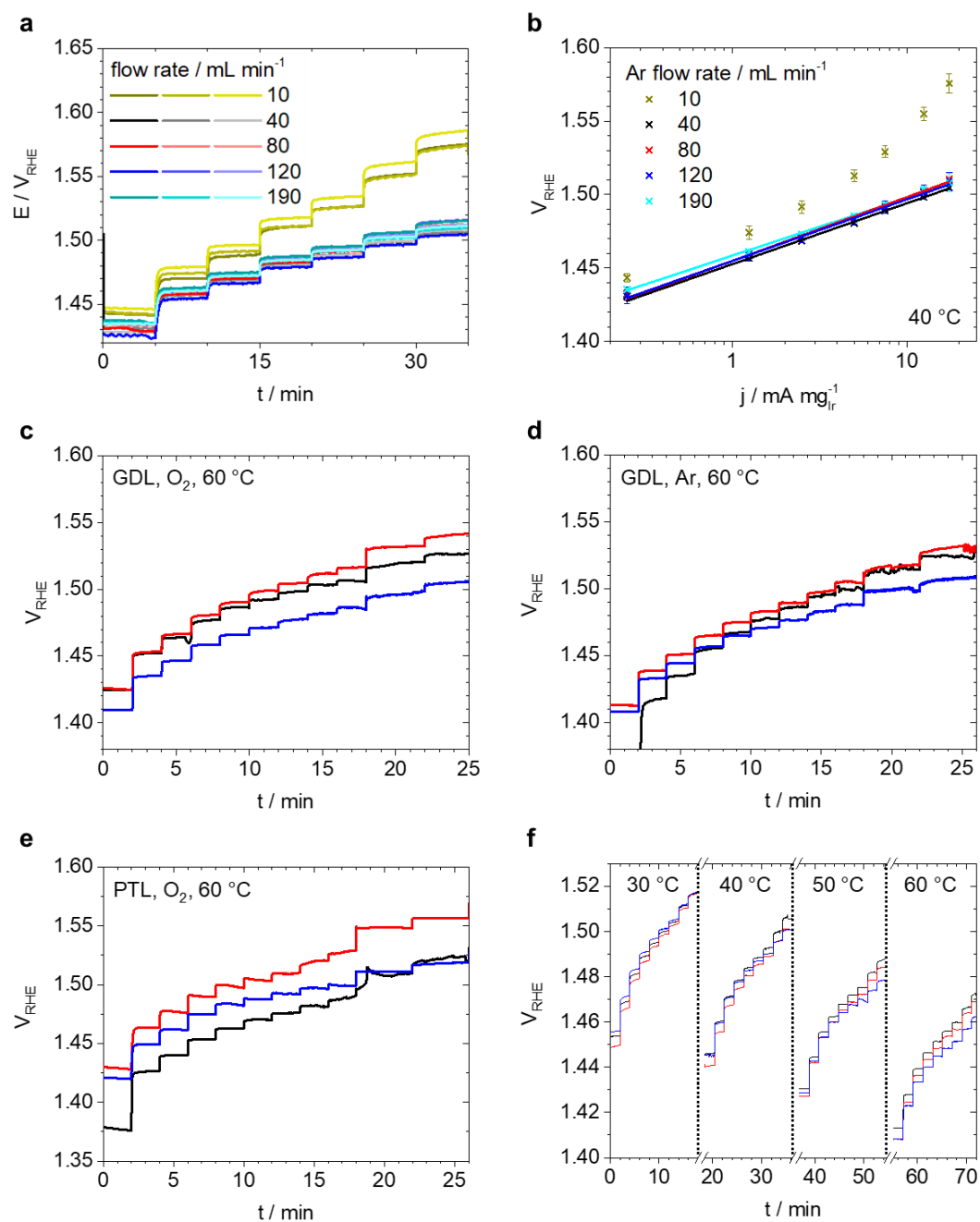


Figure S4. The three repetitions of the galvanostatic measurements of the commercial IrO<sub>2</sub> in the GDE setup applying current steps under humidified (a) Ar at different flow rates at 40 °C, (c) O<sub>2</sub> at 60 °C, (d) Ar at 60 °C, (e) O<sub>2</sub> at 60 °C using a Ti-PTL, and (f) O<sub>2</sub> in T dependent measurements (the breaks in the t axis is due to the heating up to higher T). (b) The corresponding OER mass activity  $j$  plotted of the different flow rates as Tafel plots (using the average of the  $iR$  corrected potential of the last 100 s of every step is defined as OER activity). Unless specified otherwise differently C based GDLs were used as substrate.

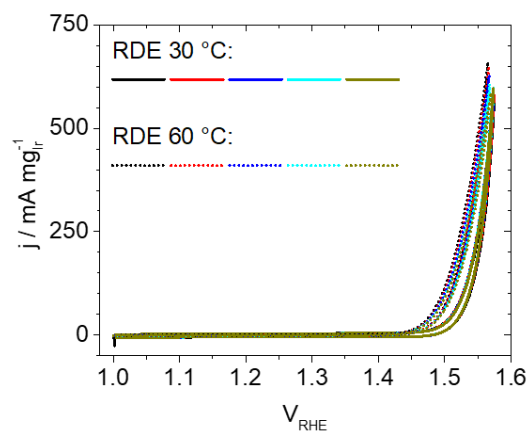


Figure S5. Five consecutive scans of linear scanning voltammetry (LSV) in RDE setup using the  $\text{IrO}_2$  catalyst at 30 °C as compared to 60 °C.

### ***Tafel plot determination***

The Tafel slope was obtained from the slopes of the linear fit in the J(E) plots. For the determination of the Tafel slope in **Error! Reference source not found.** the data of the three (GDE) repetitions (not the average of all measurements) were used. The Tafel slope at 60 °C was determined for the RDE results out of current densities between 0.8-100 mA mg<sub>Ir</sub><sup>-1</sup> and in the GDE (GDL: O<sub>2</sub> and Ar; PTL: O<sub>2</sub>) up to 40 mA mg<sub>Ir</sub><sup>-1</sup>. The deviation of the Tafel slope was obtained from the error of the slope.

The linear fits from the three repetitions in the Tafel plots were used for the determination of the activity at a certain potential.

Table S1. Tafel slopes of the GDE measurements of the IrO<sub>2</sub> catalyst depending on the flow rate, gas atmosphere, substrate, and temperature.

<b>Substrate</b>	<b>T</b> / °C	<b>Gas</b> <b>atmosphere</b>	<b>Loading</b> / mg <sub>Ir</sub> cm <sup>-2</sup> <sub>geo</sub>	<b>Flow rate</b> / mL min <sup>-1</sup>	<b>Tafel slope</b> / mV dec <sup>-1</sup>
GDL	40	Ar	4	10	-
GDL	40	Ar	4	40	40.2 ± 0.5
GDL	40	Ar	4	80	41.8 ± 0.7
GDL	40	Ar	4	120	41.9 ± 1.5
GDL	40	Ar	4	190	39.9 ± 1.0
GDL	60	O <sub>2</sub>	1	40	41.1 ± 4.8
GDL	60	Ar	1	40	50.3 ± 6.7
PTL	60	O <sub>2</sub>	1	40	44.5 ± 15.9
GDL	30	O <sub>2</sub>	1	40	45.4 ± 1.0
GDL	40	O <sub>2</sub>	1	40	41.5 ± 1.0
GDL	50	O <sub>2</sub>	1	40	38.5 ± 1.1
GDL	60	O <sub>2</sub>	1	40	40.7 ± 1.5

In the Figures 3 and 5 of the Tafel plots the average of three measurements are shown.

### ***Exchange current density and activation energy***

The linear fits from the Tafel plots of all three repeats, see Table S2, were used to determine the current density at the reversible potential. First a constant, temperature independent, reversible potential of  $E_{\text{rev}}=1.23$  V was assumed. Additionally, the temperature dependent reversible potential was determined by Parthasarathy et al.<sup>4</sup> and by an equation of Bratsch<sup>6</sup>, see Table S3. The reported exchange current densities in Table S3 are the averaged values and standard variation of the three repeats.

Table S2. Intercept and slope determined by the linear fits in the Tafel plot from the three repeats of the temperature dependent measurements in the GDE setup.

<b>T / K</b>	<b>Intercept = <math>V_{\text{RHE}}</math></b>	<b>Slope = <math>V_{\text{RHE}} \log(\text{J})^{-1}</math></b>
303.15	$1.4543 \pm 0.0011$	$0.0436 \pm 0.0011$
	$1.4515 \pm 0.0014$	$0.0450 \pm 0.0014$
	$1.4473 \pm 0.0014$	$0.0476 \pm 0.0014$
313.15	$1.4438 \pm 0.0016$	$0.0421 \pm 0.0016$
	$1.4442 \pm 0.0007$	$0.0394 \pm 0.0007$
	$1.4389 \pm 0.0010$	$0.0429 \pm 0.0011$
323.15	$1.4287 \pm 0.0012$	$0.0403 \pm 0.0012$
	$1.4261 \pm 0.0010$	$0.0399 \pm 0.0010$
	$1.4288 \pm 0.0004$	$0.0351 \pm 0.0004$
333.15	$1.4115 \pm 0.0011$	$0.0414 \pm 0.0012$
	$1.4073 \pm 0.0011$	$0.0427 \pm 0.0011$
	$1.4075 \pm 0.0006$	$0.0379 \pm 0.0007$

Table S3. The exchange current densities determined from the different reversible potentials for the four temperatures obtained from the averaged log (j) of the three repeats.

<b>Method to determine E<sub>rev</sub></b>	<b>T / K</b>	<b>E<sub>rev</sub> / V<sub>RHE</sub></b>	<b>J<sub>0</sub> / 10<sup>-9</sup> A mg<sub>Ir</sub><sup>-1</sup></b>
Parthasarathy <i>et al.</i> <sup>4</sup>	303.15	1.2224	10.6 ± 6.0
	313.15	1.2140	3.5 ± 1.8
	323.15	1.2056	2.1 ± 1.2
	333.15	1.1972	7.2 ± 3.8
Bratsch <sup>6</sup>	303.15	1.2249	12.0 ± 6.7
	313.15	1.2164	4.1 ± 2.0
	323.15	1.2080	2.4 ± 1.3
	333.15	1.1995	8.2 ± 4.3
Constant E <sub>rev</sub>	303.15	1.23	15.5 ± 8.6
	313.15	1.23	8.5 ± 4.1
	323.15	1.23	8.7 ± 4.6
	333.15	1.23	44.2 ± 20.6

Afterwards the temperature dependent Tafel plots of each repetition is used to determine log(J) at the reversible potential E<sub>rev</sub> = 0.25 V assuming a constant E<sub>rev</sub> and additionally the temperature dependent E<sub>rev</sub> values from Table S4 were used. The average of log(J) at the standard deviations of the three repeats are plotted against the inverse temperature as Arrhenius plot, see Figure S6. The product of the temperature T and the logarithm of the exchange current density log(J) was used to determine with the gas constant R the activation energy E<sub>A</sub> (in kJ mol<sup>-1</sup>) at the reversible potential by:

$$E_A = - 2.3 \cdot 10^{-3} T R \log(j)$$

The deviation of the activation energy was determined from the error of the slope “b” of the linear fit by error propagation via:

$$\left| \frac{\partial E_A}{\partial b} \right| \Delta b = \left| \frac{\partial}{\partial b} (-2.3 R b) \right| \Delta b = |-2.3 R| \Delta b$$

Table S4. Averaged values of  $\log(J)$  from the Tafel plots at an overpotential of 0.25 V using the OER overpotential from the temperature dependent measurements in the GDE setup and Arrhenius plot to determine the activation energy.

Method to determine $E_{rev}$	T / K	$\eta=0.25$ V / $V_{RHE}$	$\log(j / \text{mA mg}^{-1})$ at $\eta=0.25$ V	Arrhenius plots $\eta=0.25$ V	
				T $\log(J)$ / K	$E_A$ / $\text{kJ mol}^{-1}$
Parthasarathy et al. <sup>4</sup>	303.15	1.4724	$0.4695 \pm 0.0457$	-1492.3 $\pm 346.0$	$28.5 \pm 6.6$
	313.15	1.4640	$0.5218 \pm 0.0439$		
	323.15	1.4556	$0.7231 \pm 0.0408$		
	333.15	1.4472	$0.9479 \pm 0.0763$		
Bratsch <sup>6</sup>	303.15	1.4749	$0.5240 \pm 0.0438$	-1494.3 $\pm 338.0$	$28.6 \pm 6.5$
	313.15	1.4664	$0.5810 \pm 0.0429$		
	323.15	1.4580	$0.7855 \pm 0.0437$		
	333.15	1.4495	$1.0038 \pm 0.0786$		
Constant $E_{rev}$	303.15	1.48	$0.6370 \pm 0.0397$	-3509.7 $\pm 464.2$	$67.1 \pm 8.9$
	313.15	1.48	$0.9091 \pm 0.0385$		
	323.15	1.48	$1.3610 \pm 0.0757$		
	333.15	1.48	$1.7555 \pm 0.1123$		

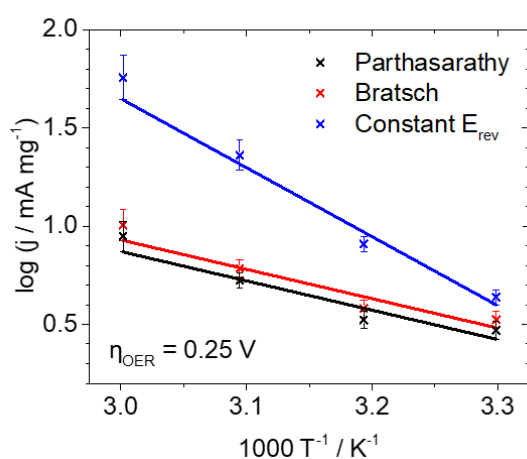


Figure S6. Arrhenius plot of the temperature dependent measurements at the OER overpotential  $\eta = 0.25$  V. The reversible potential was determined by the equation of Parthasarathy et al.<sup>4</sup> (black), Bratsch<sup>6</sup> (red), or a constant value of 1.23 V (blue) was used.



## XPS and TEM measurement

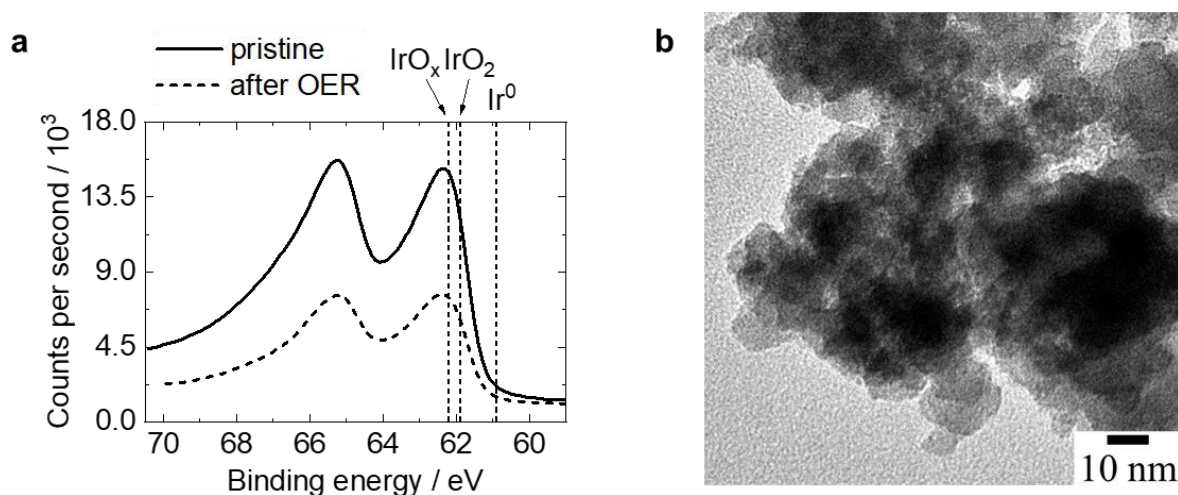


Figure S7. (a) XPS measurements of the binding energy of the IrO<sub>2</sub> catalysts, pristine (solid line) and after OER (dash line). The Ir 4f signals of Ir<sup>0</sup>, IrO<sub>2</sub>, and IrO<sub>x</sub> are marked by the black dash lines.<sup>7,8</sup> (b) TEM micrograph of the IrO<sub>2</sub> catalyst.

The XPS data of the pristine catalyst (before the activation and activity measurement) shows that the IrO<sub>2</sub> only contain iridium oxide IrO<sub>x</sub> (62.3 eV due to Pfeifer et al.<sup>7</sup>) and not metallic Ir<sup>0</sup> (60.8 eV due to Freakley et al.<sup>8</sup>), see Figure S7a. As expected after the OER performance (including the activation step before) no change in oxidation state was observed.

## References

- (1) Inaba, M.; Jensen, A. W.; Sievers, G. W.; Escudero-Escribano, M.; Zana, A.; Arenz, M. Benchmarking High Surface Area Electrocatalysts in a Gas Diffusion Electrode: Measurement of Oxygen Reduction Activities under Realistic Conditions. *Energy Environ. Sci.* **2018**, *11* (4), 988–994. <https://doi.org/10.1039/C8EE00019K>.
- (2) Yarlagadda, V.; McKinney, S. E.; Keary, C. L.; Thompson, L.; Zulevi, B.; Kongkanand, A. Preparation of PEMFC Electrodes from Milligram-Amounts of Catalyst Powder. *J. Electrochem. Soc.* **2017**, *164* (7), F845–F849. <https://doi.org/10.1149/2.1461707jes>.
- (3) Wiberg, G. K. H.; Mayrhofer, K. J. J.; Arenz, M. Investigation of the Oxygen Reduction Activity on Silver - A Rotating Disc Electrode Study. *Fuel Cells* **2010**, *10* (4), 575–581. <https://doi.org/10.1002/fuce.200900136>.
- (4) Parthasarathy, A.; Srinivasan, S.; Appleby, A. J.; Martin, C. R. Temperature Dependence of the Electrode Kinetics of Oxygen Reduction at the Platinum/Nafion®

- Interface—A Microelectrode Investigation. *J. Electrochem. Soc.* **1992**, *139* (9), 2530–2537. <https://doi.org/10.1149/1.2221258>.
- (5) Schröder, J.; Quinson, J.; Mathiesen, J. K.; Kirkensgaard, J. J. K.; Alinejad, S.; Mints, V. A.; Jensen, K. M. Ø. Ø.; Arenz, M. A New Approach to Probe the Degradation of Fuel Cell Catalysts under Realistic Conditions: Combining Tests in a Gas Diffusion Electrode Setup with Small Angle X-Ray Scattering. *J. Electrochem. Soc.* **2020**, *167* (13), 134515. <https://doi.org/10.1149/1945-7111/abdd2>.
- (6) Bratsch, S. G. Standard Electrode Potentials and Temperature Coefficients in Water at 298.15 K. *J. Phys. Chem. Ref. Data* **1989**, *18* (1), 1–21. <https://doi.org/10.1063/1.555839>.
- (7) Pfeifer, V.; Jones, T. E.; Velasco Vélez, J. J.; Massué, C.; Arrigo, R.; Teschner, D.; Girgsdies, F.; Scherzer, M.; Greiner, M. T.; Allan, J.; Hashagen, M.; Weinberg, G.; Piccinin, S.; Hävecker, M.; Knop-Gericke, A.; Schlögl, R. The Electronic Structure of Iridium and Its Oxides. *Surf. Interface Anal.* **2016**, *48* (5), 261–273. <https://doi.org/10.1002/sia.5895>.
- (8) Freakley, S. J.; Ruiz-Esquius, J.; Morgan, D. J. The X-Ray Photoelectron Spectra of Ir, IrO<sub>2</sub> and IrCl<sub>3</sub> Revisited. *Surf. Interface Anal.* **2017**, *49* (8), 794–799. <https://doi.org/10.1002/sia.6225>.
- (9) Oh, H. S.; Nong, H. N.; Reier, T.; Bergmann, A.; Gliech, M.; Ferreira De Araújo, J.; Willinger, E.; Schlögl, R.; Teschner, D.; Strasser, P. Electrochemical Catalyst-Support Effects and Their Stabilizing Role for IrO<sub>x</sub> Nanoparticle Catalysts during the Oxygen Evolution Reaction. *J. Am. Chem. Soc.* **2016**, *138* (38), 12552–12563. <https://doi.org/10.1021/jacs.6b07199>.
- (10) Oakton, E.; Lebedev, D.; Povia, M.; Abbott, D. F.; Fabbri, E.; Fedorov, A.; Nachttegaal, M.; Copéret, C.; Schmidt, T. J. IrO<sub>2</sub>-TiO<sub>2</sub>: A High-Surface-Area, Active, and Stable Electrocatalyst for the Oxygen Evolution Reaction. *ACS Catal.* **2017**, *7* (4), 2346–2352. <https://doi.org/10.1021/acscatal.6b03246>.